Adjustment of Exposure Kinetics Simulation Parameters for a 3-D Microstructure Fabrication Using Double-Exposure Lithography

Nithi Atthi[1], Patama Pholprasit[2], Thawat Thammabut[3], Wutthinan Jeamsaksiri[1], Charndet Hruanun[1], Amporn Poyai[1], and Rardchawadee Silapunt[2]

[1]*National Electronics and Computer Technology Center (NECTEC)*
[2]*King Mongkut's University of Technology Thonburi*
[3]*Western Digital (Thailand) Co.Ltd.*

E-mail addresses nithi.atthi@nectec.or.th, rardchawadee.sil@kmutt.ac.th

Abstract

This paper is focused on the adjustment of the Dill's C parameter associated with the double exposure kinetics using trial-and-error with the regression statistic. Adjusted Dill's C is used in the simulation to pattern a 3-step air bearing surface (ABS) structure. The result shows within 5.0% deviation of the remaining photoresist thickness from that of the experiment.

Keywords: Air bearing surface, Dill's parameters, Lithography simulation, Multi-exposure

1. Introduction

One of the most important components in a hard-disk drive (HDD) is the slider head which comprises a read/write head formed at the leading edge and an air bearing surface (ABS) which is aerodynamically designed to control a nanometer scale flying gap of the read/write head over the media during operation. The image of ABS on the real slider head is shown in fig.1.

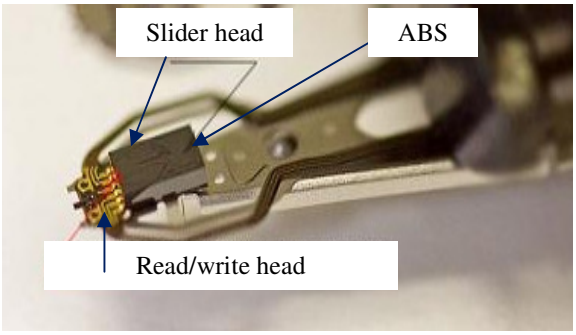

Figure 1. The components on the slider head [1].

Typically, ABS that comprises three-dimensional (3-D) microstructures can be fabricated using a multi-level lithography by varying the exposure dose (E) across the area coated with the uniform photoresist (PR) film. The exposed PR is then developed and etched in a single step to form ABS [2]. PR absorption during the exposure and its dissolution mechanism in the development step are most important input factors to the lithographic simulation that is extensively adopted for modern 3-D microstructure design [3]. In this paper, PR absorption characteristics which can be explained by Dill's 3-parameters are of interest. Dill's A (A) and Dill's B (B) are bleachable (unexposed) and non-bleachable (exposed) absorption coefficients and Dill's C (C) is the standard exposure rates constant [4]. The Dill's ABC can be expressed in terms of initial transmittance, $T(0)$, the final transmittance, $T(\infty)$, initial slope of the curve of light transmission and intensity, T_{12}, refractive index of PR (n), and PR film thickness (D). The Dill's ABC and T_{12} can be expressed as:

$$A = \frac{1}{D} ln(\frac{T(\infty)}{T(0)}) \quad (1)$$

$$B = -\frac{1}{D} ln(\frac{T(\infty)}{T_{12}}) \quad (2)$$

$$C = \frac{A+B}{AT(0)\{1-T(0)\}T_{12}} \frac{dT}{dE} | E = 0 \quad (3)$$

$$T_{12} = 1 - (\frac{n-1}{n+1}) \quad (4)$$

It can be analyzed from our previous simulation work [5] that the photochemical interaction between the 1st exposure (E_1) and the PR film is probably

occurred and causes a partial breaking of N_2 molecule bonding, thus changing the PR sensitivity during the 2nd exposure step (E_2). The PR remaining thickness (T_{PR}) of the double exposure process is apparently different from that of the single exposure (at the same total dose) as shown in fig.2. The analysis later indicates a certain change of the Dill's C parameter after the first interaction. So this paper aims to focus on an adjustment of the Dill's C parameter for the simulation to obtain more accurate results for the double exposure.

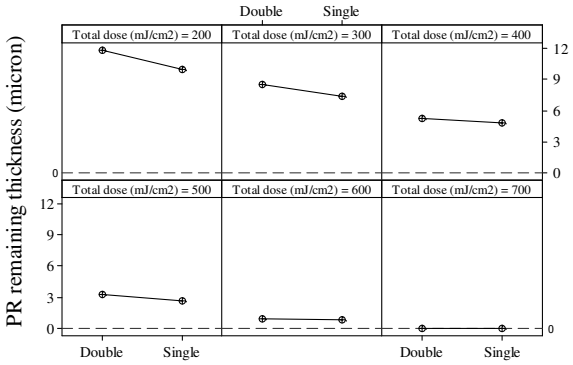

Figure 2. The plots between the PR remaining film thickness of single and double exposures.

2. Experimental Setup

The following simulation with the OPTOLITH simulator is conducted in parallel with the experiment, for comparison and validation. First, an Aluminum Titanium Carbide (AlTiC) substrate is spin coated with 20 µm thick Clariantz AZ-P4620 PR. The PR film is baked at 90˚C for 3 min. Note that, the refractive index of AZ-P4620 is n = 1.64. The 2x2 µm hole pattern is transferred to the PR film by using the Ultratech stepper with wavelength (λ) of 405 nm, Numerical aperture (NA) of 0.16, and focus distance (F) of 7.91 µm. The exposure kinetics of the PR can be explained by using the Dill's parameters from the commercial photoresist datasheet, which A = 0.3697 µm^{-1} B = 0.0243 µm^{-1}, and C = 0.0203 cm^2/mJ [6]. In the exposure step, E_1 and E_2 are varied from 50 to 500 mJ/cm^2. This means that the cumulative dose (E_c) for the double exposure is varied from 100 to 1000 mJ/cm^2. The development kinetics can be determined by Mack's model [3-4] with parameters including the dissolution rate R_{min} = 1.07x10^{-3} µm/s, R_{max} = 0.2994 µm/s, the dissolution selectivity (n) = 6.3969, and the threshold inhibitor concentration (M_{th}) = 0.1849. The exposed PR is finally spray developed by potassium hydroxide (KOH) at 23˚C for 120 sec. Finally, the T_{PR} is measured by TENCOR P-11 step profiler and the pattern image is captured by a scanning electron microscope (SEM).

3. Results and Discussion

The *Dill's C* value for the 2nd exposure is adjusted by trial-and-error until the simulated T_{PR} is relatively similar to that of the experiment as shown in fig.3. The relation between the adjusted *Dill's C* or *Dill's* C_{adj} and the exposure dose is illustrated in fig.4.

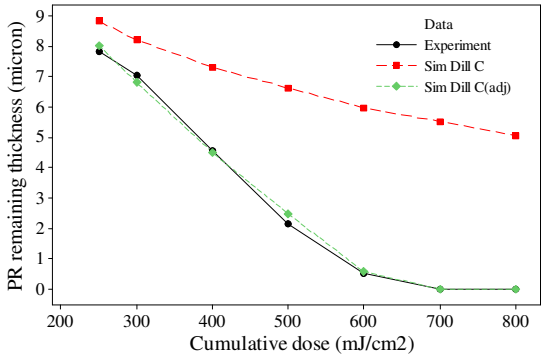

Figure 3. Simulation results of T_{PR} after the double exposure by using *Dill's* C_{adj}.

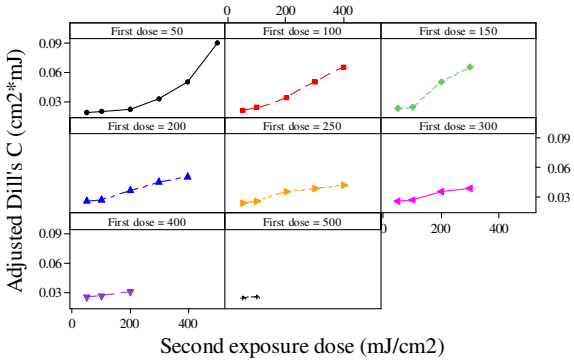

Figure 4. The relation between the adjusted *Dill's C* and double exposure dose.

These relations can be fitted by the regression plots. For the double exposure with E_1 = 50 mJ/cm^2, E_2 for a target adjusted Dill's C parameter (C_{adj}) can be predicted by the quadratic regression equation; $C_{adj} = A(E_2)^2 + B(E_2) + C$. As $E_1 \geq 50$ mJ/cm^2, E_2 for a target C_{adj} can be predicted by the linear regression equation; $C_{adj} = B(E_2) + C$. The C_{adj} predicted equation when the E_1 is 50, 100, 150, 200, 250, 300, 400, and 500 mJ/cm^2 are shown in Eq. (5) to Eq. (12). Note that, the R^2_{adj} for Eq. (5) to eq. (11) are 98.5%, 97.3%, 94.7%, 98.5%, 94.7%, and 95.9%, respectively.

$$C_{adj(50)} = 10^{-6}E_2^2 - (1.39x10^{-4})E_2 + 2.58x10^{-2} \quad (5)$$

$$C_{adj(100)} = (1.31x10^{-4})E_2 + 1.07x10^{-2} \quad (6)$$

$$C_{adj(150)} = (1.87x10^{-4})E_2 + 9.59x10^{-3} \quad (7)$$

$$C_{adj(200)} = (7.60x10^{-4})E_2 + 2.07x10^{-2} \quad (8)$$

$$C_{adj(250)} = (5.40x10^{-5})E_2 + 2.15x10^{-2} \quad (9)$$

$$C_{adj(300)} = (5.40x10^{-5})E_2 + 2.26x10^{-2} \quad (10)$$

$$C_{adj(400)} = (3.40x10^{-5})E_2 + 2.40x10^{-2} \quad (11)$$

$$C_{adj(500)} = 2.53x10^{-2} \quad (12)$$

The comparison of the simulation images of the 2x2 μm hole pattern on the PR film using normal Dill's C (0.0203 cm^2/mJ) and adjusted Dill's C (C_{adj}) from Eq. (5) to Eq. (12) are shown in fig.5.

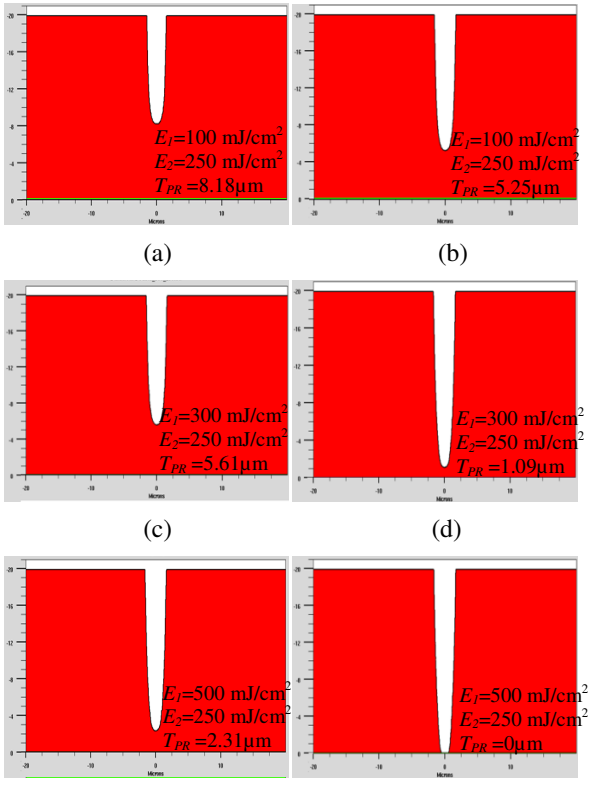

Figure 5. Simulation results of 2x2 μm hole patterns: (a), (c), (e) normal Dill's *C* and (b), (d), (f) adjusted Dill's *C*.

To verify *Dill's* C_{adj}, the AlTiC coated with 20 μm of AZ-P4620 PR is exposed by fixing the 2nd exposure dose (E_2) at 250 mJ/cm^2 and varying the condition of the 1st exposure dose (E_1) at 100, 300, and 500 mJ/cm^2. The exposed PR is developed by KOH for 120 sec. Then the T_{PR} is measured. The SEM images in fig.6 (a) and (b) show that some PR films is remained on the AlTiC substrate when the cumulative exposure doses (E_c) are 350 and 550 mJ/cm^2, respectively. However, when E_c is increased to 750 mJ/cm^2, the PR film is fully exposed and completely dissolved in the KOH developer as shown in fig.6 (c). Moreover, the T_{PR} measured from the simulation using C_{adj} is similar to one measured from the experiment.

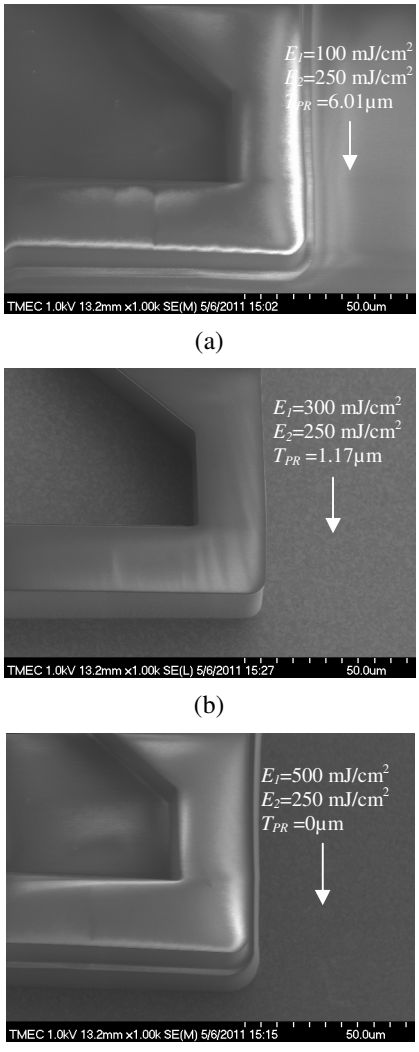

Figure 6. SEM image of PR pattern using various cumulative dose; (a) 350 mJ/cm^2, (b) 550 mJ/cm^2, and (c) 750 mJ/cm^2.

The normal Dill's *C* from the PR datasheet and *Dill's* C_{adj} are applied for the 3-D pattern simulation. The 3-step ABS structure is fabricated by using the exposure condition from the simulation. The schematic layout of the ABS design is shown in fig.7 with the initial PR thickness of 20 µm and the target PR thicknesses at the position S_1, S_2, and S_3 are 16, 10, and 8 µm, respectively. The single exposure doses for S_1 and S_2 position are 50 and 200 mJ/cm^2 respectively, and the double exposure dose (E_1+E_2) for S_3 position is (200+50) = 250 mJ/cm^2. The exposed PR is finally spray developed by KOH at 23˚C for 120 sec.

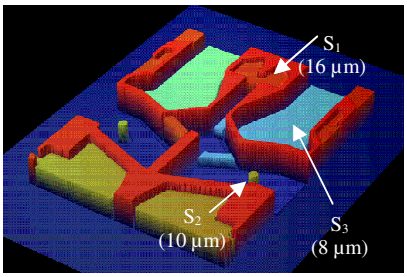

Figure 7. The 3-D schematic layout for 3 steps height of ABS structure.

The simulated T_{PR} at S_1, S_2, and S_3 are determined as 16.30 µm, 9.64 µm, and 8.02 µm, respectively (see fig.8). The differences between simulated and target T_{PR} at S_1, S_2, and S_3 are ±1.88%, ±3.60%, and ±0.25%, respectively. Note that, the actual T_{PR} is normally controlled within ±5% of the target.

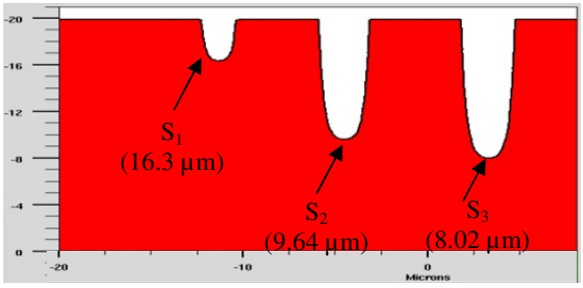

Figure 8. The simulation images after the development at 3 positions of the ABS structure.

The 45˚ tilted SEM image of the ABS structure using the exposure condition from the simulation is shown in fig.9. The actual T_{PR} at S_1, S_2, and S_3 are 16.14 µm, 9.99 µm, and 7.82 µm, respectively. The errors between simulated T_{PR} and actual T_{PR} are then ±0.99%, ±3.50%, and ±2.56% respectively, which are only ±3.5% in maximum. The errors between actual T_{PR} and target T_{PR} are ±0.87%, ±0.10%, and ±2.30% respectively, the average is maintained within ±5.0%.

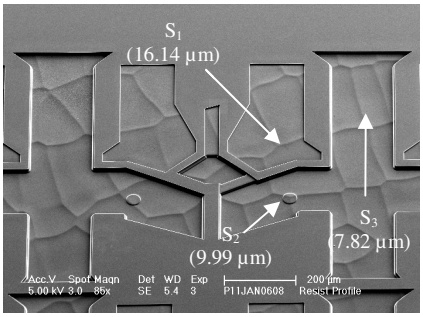

Figure 9. SEM image of ABS structure fabricated using the simulated condition.

4. Conclusions

The accuracy of the simulation model of the double exposure lithography for the ABS is improved by adjusting the *Dill's C* parameter. This compensated *Dill's C* can be fitted by sets of regression equations for different exposure doses. The simulated exposure condition is experimentally validated within ±5.0% difference thus this simulation model can be a potential approach for a 3D microstructure fabrication.

5. Acknowledgment

The authors would like to thanks all staffs from Western Digital (Bang Pa-In) Thailand and Thai Microelectronics Center (TMEC) for their support.

References

[1] http://en.rlab.ru/doc/. Available on 10 May 2011.

[2] N. Atthi, J. Jantawong, W. Jeamsaksiri, C. Hru-anun, and A. Poyai, "3-dimensionals lithography techniques for air bearing surface patterning in Hard-disk drive reading/writing head manufacturing", Khon kaen University Research Journal, 13 (3), pp. 353-359, 2008.

[3] S-K. Kim, J-E. Lee, S-W. Park, H-K. Oh, "Optical lithography simulation for the whole resist process", Current Applied Physics, 6, pp. 48–53, 2006.

[4] W. Flack and G. Newman, "Advanced Simulation Techniques for Thick Photoresist Lithography", SPIE 3049-72, pp. 1-16, 1997.

[5] P. Pholprasit, N. Atthi, T. Thammabut, W. Jeamsaksiri, C. Hruanun, A. Poyai, and R. Silapunt, "Double Exposure Effects on Photoresist Model Parameters in 3-D Patterning", ITC-CSCC, 2011. To be published.

[6] www.az-em.com/twn/PDFs/p4000/az_p4000.pdf. Available on 10 May 2011.